

Double Metal Cyanide Complexes Synthesized by Solvent-Free Grinding Method for Copolymerization of CO₂ and Propylene Oxide

Wuyuan Zhang, Qiang Lin, Yi Cheng, Lingbin Lu, Bo Lin, Lisha Pan, Nai Xu

Key Laboratory of Ministry of Education for Application Technology of Chemical Materials in Hainan Superior Resources, School of Materials and Chemical Engineering, Hainan University, Haikou, Hainan 570228, China

Received 7 February 2011; accepted 21 March 2011

DOI 10.1002/app.34544

Published online 9 August 2011 in Wiley Online Library (wileyonlinelibrary.com).

ABSTRACT: Two active double metal cyanide (DMC) complexes were successfully synthesized by solvent-free grinding method. Their structures were characterized by FTIR spectrometer and X-ray diffractometer. The results showed that Complex 1 (double metal cyanide complex with K₃Fe(CN)₆ and ZnCl₂) and Complex 2 (double metal cyanide complex with K₃Fe(CN)₆ and Zn(CH₃COO)₂) had the same structures, crystal forms, and lower crystallinity as both of them synthesized by conventional solvent-based methods, respectively. Investigations on grinding conditions indicated that Complex 1 ground 14 min at a high grinding strength could achieve low crystallinity and showed substantially amorphous structures. Two speculated structures

of DMC were given. The alternating copolymerization of CO₂ and propylene oxide with Complex 1 as catalyst obtained anticipated poly(propylene carbonate) (PPC) with very high catalytic activity. The PPC produced by optimized Complex 1 has molecular weight (M_n) up to 98,000 and narrow polydispersity of 1.93 with more than 90% carbonate linkages. Compared with Complex 1, Complex 2 displayed low catalytic activity but high selectivity mainly due to the electron atmosphere and strong steric hindrance. © 2011 Wiley Periodicals, Inc. *J Appl Polym Sci* 123: 977–985, 2012

Key words: carbon dioxide fixation; double metal cyanide; solvent-free grinding; copolymerization; polycarbonates

INTRODUCTION

Carbon dioxide (CO₂) has seriously been considered to be a greenhouse gas causing the global warming that may lead to great change in climate.^{1–3} The fixation of CO₂ to polymeric materials for the application in industrial fields is one of the most valuable researches for the 21st century considering the environmental issues.^{4,5} Inoue first showed that partially hydrolyzed ZnEt₂ initiated the copolymerization of propylene oxide (PO) and CO₂.^{6,7} Now the copolymerization has been one of the topics recently studied intensively in the polymer science for biodegradable polymeric materials and utilization of greenhouse gas.⁸ As a result of these research efforts, a number of catalyst systems have been developed.^{9–40} Noticeably, high sterically hindered catalysts such as

[(BDI)ZnOAc] complexes,^{22–28} chromium-salen complexes,^{29–32} and cobalt-salen complexes,^{33–36} which have been invented in recent years, show high activity in the copolymerization of CO₂ and epoxides. These systems can initiate the reactions even under mild conditions and in some cases allow for the regio- or stereo-selective polymerization, with high molecular weight and narrow polydispersity of the products. However, synthesis of these newly-developed catalysts is so complex that it is difficult to manufacture in common laboratory or plant.

The DMC complexes discovered in the early 1960s by General Tire are very effective for CO₂ and PO polymerization (44 g g⁻¹ cat., based on Zn₃Fe(CN)₆).^{37,39} Furthermore, DMC complexes show desirable properties with regard to greater storage stability, catalyst longevity, simple synthesis process, and multi-use.^{37–41} The DMC also showed a potential application in terpolymerization of CO₂, epoxides and acid anhydrides or inner esters (e.g., γ -butyrolactone), the glass-transition temperature (T_g) and degradability of the products could be highly improved.⁴² However, the conventional solvent-based synthesis of DMC was characterized by time-, energy-, and materials-consuming. For instance, in the US Patent 5,900,384, over 100 h would be taken to prepare DMC in solution.⁴¹ Therefore, seeking for simplified process to synthesize DMC is meaningful and promising.

Correspondence to: L. Lu (lulingbin@126.com).

Contract grant sponsor: Key Scientific and Technical Project of Hainan Province; contract grant number: 090502.

Contract grant sponsor: Project of Scientific and Technical Personnel Server for Enterprises; contract grant number: 2009GJE20014.

Contract grant sponsor: Science and Technology Innovation Platform for Graduate of Hainan University.

In this article, two DMC complexes were synthesized by the mechanochemical method without solvent. Complex **1** was obtained by ball milling potassium hexacyanoferrate(III) and zinc chloride; Complex **2** was obtained by milling potassium hexacyanoferrate(III) and zinc acetate. The work provides a novel method to obtain active DMC and to really improve the efficiency of DMC synthesis.

EXPERIMENTAL

Materials

Carbon dioxide (purity more than 99.9%), potassium hexacyanoferrate(III) [$K_3Fe(CN)_6$], zinc chloride ($ZnCl_2$), zinc acetate [$(CH_3COO)_2Zn$], and *tert*-butyl alcohol (*t*BuOH), were analytical purity and directly used unless otherwise mentioned. Propylene oxide (PO) was analytical purity and immersed in 4 Å molecular sieves for 2 days before use.

Methods

Synthesis of DMC

Reaction conditions involved a mol ratio 10 : 1 mixture of $ZnCl_2/(CH_3COO)_2Zn$ and $K_3Fe(CN)_6$, ground with a Spex 8000M shaker mill in a 65-mL stainless steel vessel with two 12.70 mm and four 6.35 mm steel balls at 50 Hz for the specified time. After the reaction is finished, products were washed with 30 mL mixed solution of de-ionized water, and *t*BuOH so as to remove excess reactants and introduce the required complexing agent. The final precipitates were dried under vacuum at 50°C till constant weight. For comparison, the DMC was also synthesized following the conventional ways according to the literature.^{38,39}

Copolymerization

Copolymerization of CO_2 and PO was carried out in a 500-mL steel autoclave equipped with a magnetic stirrer, water bath heating, and a check valve. Dried DMC was added into the autoclave, followed by adding a desired amount of purified PO under vacuum conditions. The autoclave was pressurized to 3.8 MPa with CO_2 . Then the autoclave was heated at 60°C with stirring. After 40 h, the autoclave was cooled down to room temperature, slowly depressurized, and opened. The obtained polymer products were dissolved in acetone, stirred for 15 min, then poured into water, isolated, and dried under vacuum at 55°C.

Characterization

The microstructure of DMC was investigated and compared with that of solvent-based DMC by

Bruker FTIR spectrometer (Model: TENSOR 27) with 32 scans per experiment at a resolution of 1 cm^{-1} . X-ray diffraction measurement of DMC was performed on a Bruker AXS/D8 Advance diffractometer using Cu $K\alpha$ radiation at 40 kV and 30 mA. The data were collected from 1.5° to 60° 2θ with a step size of 0.025° 2θ and a counting time of 0.5 s per step. Transmission electron microscopy (TEM) pictures were taken using JEM 2100 transmission electron microscope, using an acceleration voltage of 200 kV. Samples were suspended in absolute ethyl alcohol and spread on copper grids coated with Fromwar foil.

Spectroscopic analyses of polymer products were performed using the Bruker FTIR spectrometer and a Bruker NMR spectrometer (Model: Bruker AV 400 MHz) with 1H and ^{13}C probes, $CDCl_3$ as the solvent. Number average molecular weight (M_n) and polydispersity index (PDI) of polymer products were estimated using a gel permeation chromatography (GPC) system (Waters HPLC Pump, Waters 1515 detector) with a set of three columns (Waters Styragel 500A, 10,000A and 100,000A). The GPC system was calibrated by a series of polystyrene standards with polydispersities of 1.02 supplied from Shodex. Tetrahydrofuran (THF, HPLC grade) was used as an eluent.

RESULTS AND DISCUSSION

Characterization of DMC

The preparation of DMC started from the mechanochemical reactions between $K_3Fe(CN)_6$ and ZnX_2 ($X = Cl, CH_3COO-$) by solvent-free grinding. According to the investigation, an excess of zinc salts guaranteed complete conversion and gave high catalytic activity. Complexes **1** and **2** synthesized by grinding revealed characteristic absorption peaks in FTIR spectrums basically similar to that prepared in solution, respectively. The FTIR spectra of Complex **1** exhibited characteristic peaks attributed to the $C\equiv N$ stretching absorption in the $Zn^{2+}-CN-Fe^{3+}$ unit at 2100 cm^{-1} , and Fe-CN flexural vibration absorption at 600 cm^{-1} , 496 cm^{-1} (shown in Fig. 1). And because of existing in complexing agent *t*BuOH, the $-OH$ in Complex **1** showed a broad band assigned to stretching vibration absorption at 3500 cm^{-1} , C-H stretching vibration absorption peak appeared at 2930 cm^{-1} . Owing to the coordination of Zn^{2+} with $C\equiv N$, the $C\equiv N$ bond was weakened and a resembling $C=N$ bond formed in the $Zn^{2+}-CN-Fe^{3+}$ unit of DMC, which showed a symmetric stretching vibration absorption peak at 1619 cm^{-1} .

The FTIR spectra of Complex **2** in Figure 2 exhibited characteristic peaks of $C\equiv N$ stretching absorption at 2100 cm^{-1} , Fe-CN flexural vibration

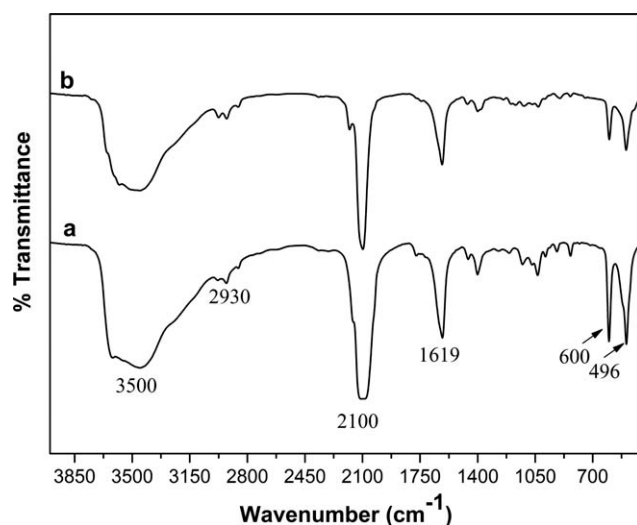


Figure 1 Comparisons of FTIR spectra of Complex 1: (a) grinding synthesis; (b) solvent synthesis.

absorption at 697 cm^{-1} , —OH stretching vibration absorption at 3450 cm^{-1} , C—H (from $t\text{BuOH}$ and zinc acetate) stretching vibration absorption at 2923 cm^{-1} , and C—H (from zinc acetate) flexural vibration absorption at 1440 cm^{-1} . Compared with Complex 1, Complex 2 presented a new characteristic peak assigned to $\text{C}\equiv\text{N}$ stretching absorption at 2178 cm^{-1} . Because of the property of zinc acetate, C=O antisymmetric stretching vibration absorption peak split and was detected at 1628 and 1568 cm^{-1} .

Crystallization of the dried DMC was determined by an X-ray diffractometer. The essence of DMC with high activity is amorphous, this means the lower crystallinity of DMC is, the higher its catalytic activity is.^{43–48} Figure 3 shows X-ray diffraction pattern of Complex 1 ground for 14 min had the same crystal pattern with that prepared in solution.

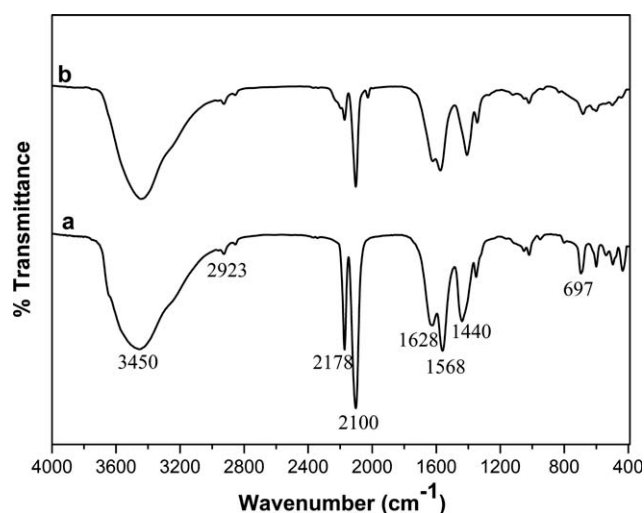


Figure 2 Comparisons of FTIR spectra of Complex 2: (a) grinding synthesis; (b) solvent synthesis.

Typically, Complex 1 ground for 14 min is substantially amorphous according to the substantial absence of sharp lines in the XRD patterns, displaying very broad peaks not associated with any sharp peaks between 2θ values of 13.5° and 22.5° and $2\theta = 23.6^\circ$. Results of copolymerization of CO_2 and PO in Table I implied that Complex 1 ground 14 min exhibited the highest catalytic activity. Grinding conditions were observed when grinding time and strength were taken as the control parameters based on the kinetic model showing fundamental factors which influence the mechanochemical reactions.^{49,50} In Figure 3, Complex 1 ground 11 min displayed sharp and dense peaks, exhibiting higher crystallinity and lower catalytic activity mainly due to incomplete transformation of the reactants within shorter mill time. Complex 1 ground 14 and 18 min showed significantly broadened peaks at about $2\theta = 23.6^\circ$, suggesting a much smaller crystallite size and/or a lowering of the crystallinity, respectively. Crystal intensity of diffraction peaks greatly increased with grinding time prolonging from 24 to 30 min, exhibiting two sharp peaks at $2\theta = 17.4^\circ$, 24.5° , respectively. At much more longer grinding (40 min), the crystallinity seems to be constant. Yield of the copolymerization of CO_2 and PO was relatively low when longer ground Complex 1 was used (shown in Table I). These results demonstrate that the grinding time has an important impact on the crystallite size and crystallinity of DMC, which may strongly affect the catalytic activity.

Figure 4 indicated that Complex 1 ground 14 min at a highest grinding strength by placing 12.70 mm and four 6.35 mm steel balls was poorly crystalline, compared with those ground at a lower or lowest strength by decreasing the number and size of the

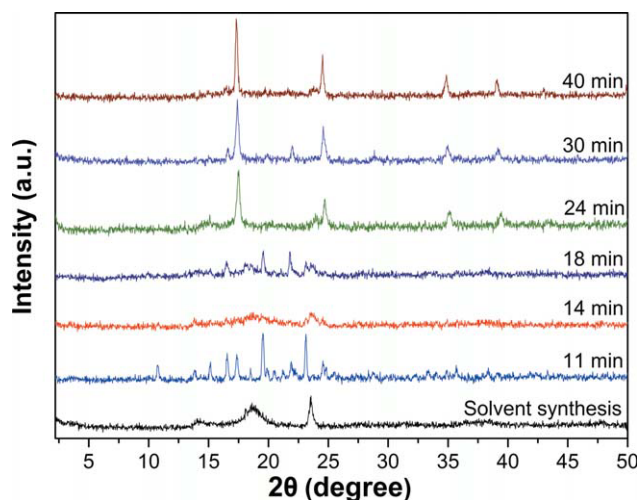


Figure 3 Comparisons of XRD patterns of Complex 1 synthesized at 50 Hz for the specified time. Two 12.70 mm and four 6.35 mm steel balls were placed. [Color figure can be viewed in the online issue, which is available at [wileyonlinelibrary.com](http://www.interscience.wiley.com).]

TABLE I
Results of PO and CO₂ Copolymerization with Ground DMC as Catalysts^a

Entry	Complex	Grinding time ^b (min)	TON ^c	TOF ^c	Selectivity ^d (% PPC)	M _n /M _w /PDI ^e	f(CO ₂) ^f
1 ^g	1	/	417.94	10.75	89.0	71 k/165 k/2.33	0.37
2	1	11	249.20	6.23	78.3	43 k/136 k/3.16	0.29
3	1	14	773.54	19.34	91.0	98 k/190 k/1.93	0.40
4	1	18	455.03	11.38	88.5	83 k/179 k/2.15	0.38
5	1	24	259.79	6.50	81.3	50 k/130 k/2.57	0.36
6	1	30	271.96	6.80	83.0	58 k/158 k/2.73	0.33
7	1	40	240.36	6.01	80.7	33 k/119 k/3.61	0.25
8 ^g	2	/	229.34	5.73	95.0	123 k/209 k/1.70	0.43
9	2	7	240.42	6.01	95.0	140 k/229 k/1.63	0.44

^a Copolymerization reactions of CO₂ (3.8 MPa) and PO (100 mL) using DMC (0.6 g) were carried out at 60°C for 40 h without solvent.

^b Synthesis reactions of DMC were carried out for the specified time at 50 Hz.

^c Turnover number in g-polymer/g-Zn and Turnover frequency in g-polymer/g-Zn h.

^d Determined by using ¹H NMR spectra.

^e Determined by gel permeation chromatography relative to polystyrene standards in tetrahydrofuran.

^f CO₂ content in copolymer, which was determined by ¹H NMR spectra.

^g DMC prepared in the conventional solvent-based ways.

balls. The results demonstrate that a stronger grinding strength would contribute to low crystallinity and high catalytic activity. Therefore, Complex 1 ground 14 min at 50 Hz is the optimal conditions for solvent-free synthesis.

Interestingly, grinding time and strength played a really unobvious role in inducing chemical reactions and phasing transformation for solvent-free synthesis of Complex 2. The 2 ground 7 min could reach complete reaction and displayed XRD pattern as shown in Figure 5; longer grinding or lower strength seemed to have no effect on the crystal pattern according to the experiment. Yield of Complex

2 was low (Table I, Entry 9) mainly due to the electron atmosphere and strong steric hindrance of the different chemical bonding in DMC structures.

Proposed mechanism of reactions in grinding process

The possible reaction mechanism in the grinding process is deduced that, ZnX₂ and K₃Fe(CN)₆ in the vessel were strongly ground and collided by steel balls, their size diminished along with specific surface area increased.⁵¹ As a result, surface defects and dislocations of K₃Fe(CN)₆ and ZnX₂ gradually generated.⁵² At the same time, some of the partial

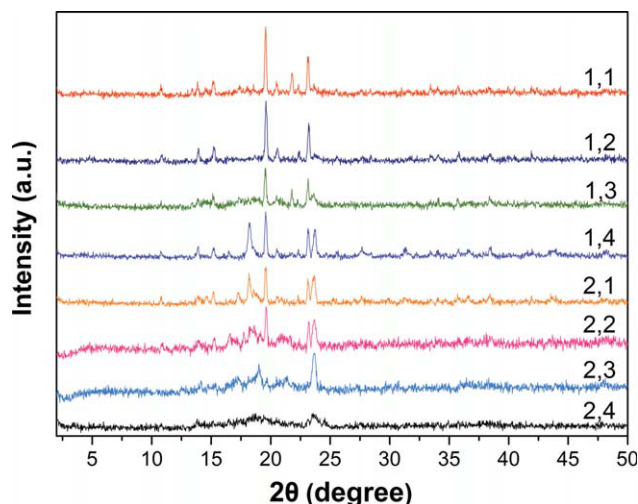


Figure 4 Comparisons of XRD patterns of Complex 1 synthesized at 50 Hz for 14 min. Grinding strength versus ball size and number; (2,4) means two 12.70 mm and four 6.35 mm steel balls, and so forth. [Color figure can be viewed in the online issue, which is available at wileyonlinelibrary.com.]

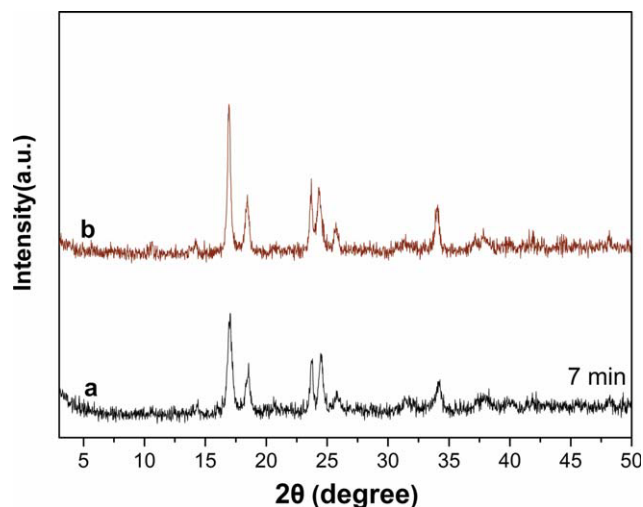


Figure 5 Comparisons of XRD patterns of Complex 2. (a) Grinding synthesis at 50 Hz for 7 min. Two 12.70 mm and four 6.35 mm steel balls were placed. (b) Solvent synthesis. [Color figure can be viewed in the online issue, which is available at wileyonlinelibrary.com.]

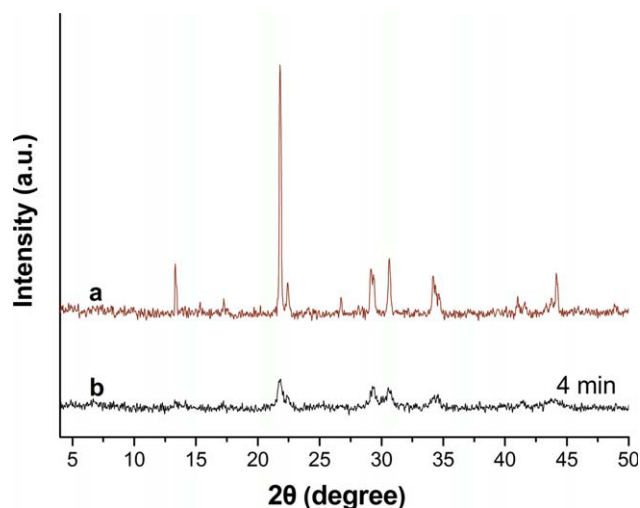


Figure 6 XRD patterns of (a) pure $\text{K}_3\text{Fe}(\text{CN})_6$ and (b) $\text{K}_3\text{Fe}(\text{CN})_6$ ground 4 min at 50 Hz. [Color figure can be viewed in the online issue, which is available at wileyonlinelibrary.com.]

collision points got a higher temperature and more energy could be stored in the defects and dislocations.⁵³ Therefore, mechanochemical activity points formed. As the ball milling process continuously carried out, the caused defects and dislocations dispersed, and part of the bonds of both $\text{K}_3\text{Fe}(\text{CN})_6$ and ZnX_2 broke and Zn atoms partially rearranged.^{49,50} Eventually, the grinding process would lead to thermal chemical reaction in the nanometer scale between $\text{K}_3\text{Fe}(\text{CN})_6$ and ZnX_2 .^{54,55} This can be partly explained by the fact that pure $\text{K}_3\text{Fe}(\text{CN})_6$ ground 4 min tended to be an amorphous structure as shown in Figure 6. And amorphization raises the free energy of the solid compared to the crystalline state, which would help in atoms reorganization as widely observed.⁵⁶

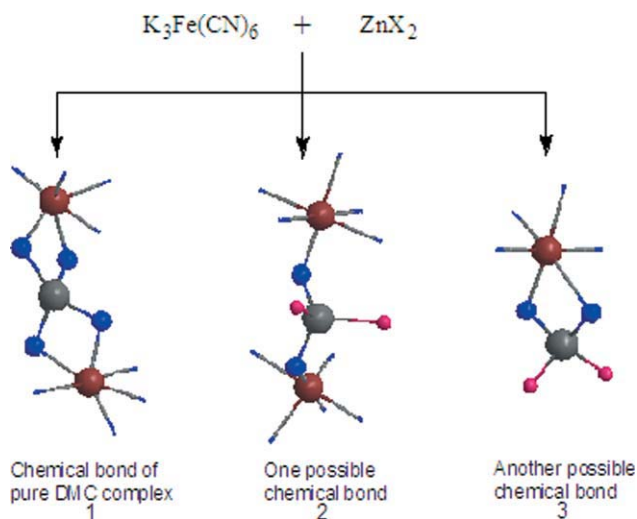
Speculated structures of DMC

For the hardness to get single crystal and other convincing evidences, the structure of DMC has not been fully established yet. Verdaguer partially determined and regarded the DMC as Structure 1 in Scheme 1; Zn atom was surrounded by four coordinated Zn–N bonds.⁵⁷ Kim et al. investigated pyridine-zinc-halide system used for CO_2 and PO polymerization and obtained the in-process product of both complex and polymer monomer, which were determined by a single crystal diffraction test.⁵⁸ Finally they confirmed Zn–N bond as the active center. With provision for the DMC with similar chemical structure of the system, the Zn–N bond is deduced to be the active center of DMC. Herein, two more speculated structures based on the above findings and experimental results were given as Structures 2 and 3 in Scheme 1. Obvious evidences

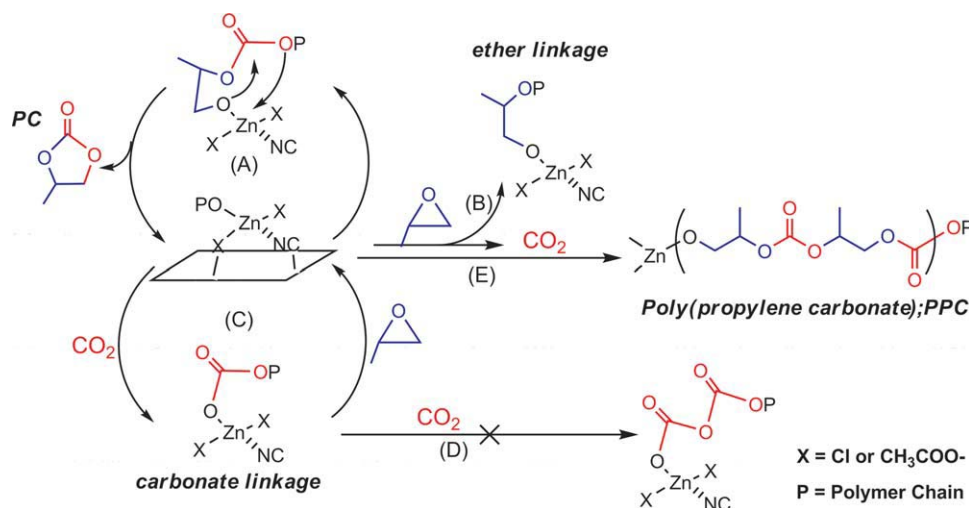
are shown as following: (1) characteristic absorption peaks of Complex 2, with organic ligand (CH_3COO^-) of zinc acetate, were detected in FTIR spectrum (Fig. 2), 1628 and 1568 cm^{-1} (C=O anti-symmetric stretching), 1440 cm^{-1} ($-\text{CH}_3$ flexural vibration) and 1020 cm^{-1} (C–O symmetric stretching). It demonstrates the coordination of CH_3COO^- in DMC structure. (2) The fact that Figures 3 and 5 gave two different patterns and diffraction peaks, negating the hypothesis that Complexes 1 and 2 with Zn atom completely coordinated with nitrogen atoms as Structure 1 should have the same crystal patterns. Thus, it can be concluded that the centric Zn^{2+} are coordinated with not only nitrogen atoms but also negative ions, such as Cl^- and CH_3COO^- . The decrease of spatial hindrance may contribute to giving Structures 2 and 3.

Copolymerization of CO_2 and PO

The Zn–N bond was suggested to play a crucial role in initiation and chain propagation of the polymerization.^{57,58} The ferrum(III)-cyano-group coordinating to the active Zn^{2+} center transfers to the propagating metal polymer chain, thereby labilizing the Zn–N bond and facilitating the PO insertion; and CO_2 enchainment might be partly enhanced by the electron-rich Zn^{2+} centers, resulting in ready increase of CO_2 content in the copolymer.^{48,59–61} Based on the polymerization results, proposed mechanism of CO_2 and PO copolymerization employing ground DMC with Structure 2 is depicted in Scheme 2. Pathway A producing both carbonate backbone and cyclic carbonate (PC) at the surface of



Scheme 1 Solvent-free grinding synthesis for DMC. Centric Zn atom is shown in dark gray, Fe in dull red, N in blue, and X (Cl or CH_3COO^-) in pink. [Color figure can be viewed in the online issue, which is available at wileyonlinelibrary.com.]



Scheme 2 Proposed copolymerization scheme of PO and CO₂ at the surface of ground DMC as catalyst with Structure 2. [Color figure can be viewed in the online issue, which is available at wileyonlinelibrary.com.]

DMC is expected to be enhanced by the electron-rich Zn²⁺ center, while Pathway B leading undesired ether linkages could not be repressed due to kinetically controlled homopolymerization. This can be confirmed by reasonable amount of PC and polyether produced in copolymerization of PO and CO₂. The relative importance of Pathway C producing biodegradable carbonate linkages over A is expected to be dependent on the steric and electronic environments of the metal center. This can be explained by the selectivity of Complexes 1 and 2. Typically, Pathway D is an impossible way to get perfect alternating copolymer with absolute CO₂ by using the catalysts of the present study. Pathway E mainly has a head-to-tail sequence and a random distribution of configurational sequences to produce PPC.^{59,62} Results of PO and CO₂ copolymerization shown in Table I indicated the importance of Pathways A, B, and C. Complex 2 showed surprisingly high selectivity probably due to the strong steric hindrance from coordinated carboxyls (when X = CH₃COO⁻ in Scheme 2) and the electron atmosphere.

Analysis of copolymer

The extent of carbonate and ether backbone could be easily traced by FTIR and NMR spectroscopies of the copolymers. As shown in Figure 7, the intense C=O antisymmetric vibration absorption peaks appear at ~ 1750 cm⁻¹. Together with this, the existence of absorption peaks around 1260 cm⁻¹, which is assigned to C—O stretching vibration absorption, provides an evidence for the presence of both carbonate and ether backbone in the resultant copolymers.

All isolated copolymers were subjected to ¹H and ¹³C NMR analyses in CDCl₃, and a representative spectrum of the PPC is shown in Figures 8 and 9,

respectively. The ¹H NMR spectrum of PPC produced by Complexes 1 and 2 showed 91%, 95% carbonate linkages, respectively. The ¹³C NMR spectrum of the PPC produced by Complexes 1 and 2 showed head-to-head, head-to-tail, and tail-to-tail linkages in the ratio 16.8 : 72.3 : 10.9, 16.7 : 76.0 : 7.3, respectively. Such a microstructure is consistent with a near random ring-opening of PO and is similar to polymers catalyzed by [(BDI)ZnOAc] complexes (~ 54% head-to-tail linkages)²⁴ and zinc glutamate (~ 60% head-to-tail linkages).⁶²

Catalytic activity of DMC

The ground DMC exhibited high efficiency in the polymerization reaction, and far higher than conventional solvent-based ones.³⁸ Complex 1 exhibited higher catalytic efficiency than Complex 2, while the

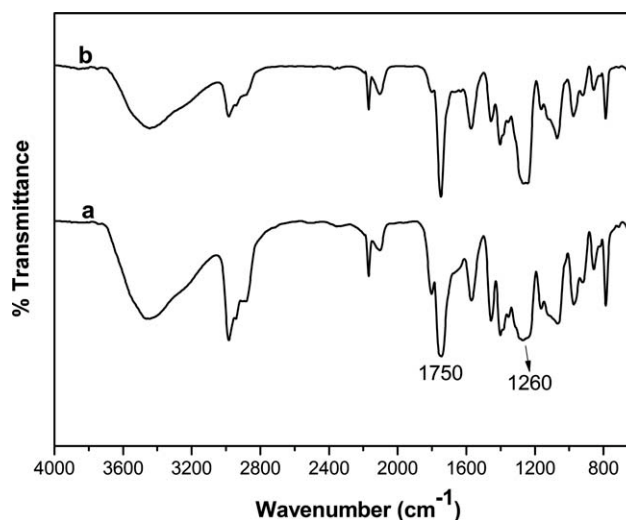


Figure 7 FTIR spectra of poly(propylene carbonate) produced by (a) Complex 1 and (b) Complex 2.

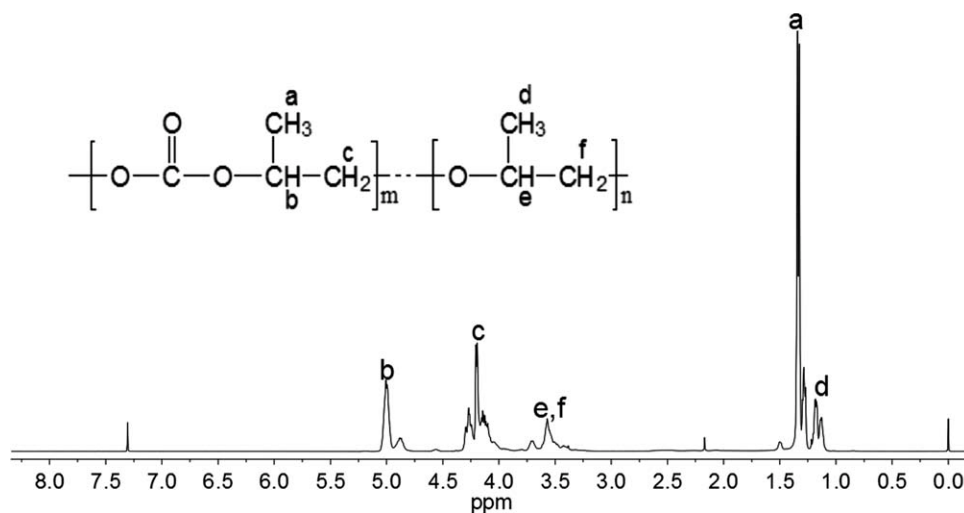


Figure 8 ^1H NMR spectrum of a representative sample of poly(propylene carbonate).

copolymerization product produced by Complex 2 gave better properties by showing higher M_n (140 K), narrower PDI (1.63), and more content of CO_2 (44%) (shown in Table I). As discussed earlier, main reasons of the results are that negative ions of zinc salts have a great impact on electron atmosphere in Zn^{2+} center, as well as spatial hindrance. The order of electronegativity is $\text{Cl}^- > \text{CH}_3\text{COO}^-$. The electron atmosphere of Zn^{2+} center centralizes to $\text{Zn}-\text{Cl}$ bond and attenuates the binding force of the active $\text{Zn}^{2+}-\text{CN}-\text{Fe}^{3+}$ unit when X of the DMC is Cl^- ; such a change would facilitate the break of $\text{Zn}-\text{N}$ bond and the PO insertion. While the X is CH_3COO^- , the electron atmosphere of Zn^{2+} center centralizes less than to $\text{Zn}-\text{Cl}$ bond, leading a stronger binding force of the active $\text{Zn}-\text{N}$ bond. Meanwhile, spatial hindrance increased when the X is

CH_3COO^- , making it difficult for PO insertion but increasing the selectivity for desired polymer up to 95% (see Table I).

Particle size of DMC using a grinding method was in the range of 20–100 nm as shown in Figure 10. Complex 1 ground 14 and 24 min showed the smallest size (~ 50 nm) [Fig. 10(b,c)] compared with those synthesized in solution about 750 nm [Fig. 10(a)], $2.93 \mu\text{m}$ (D_{50}) by using spray drier⁴¹ and 100 nm using an emulsifier.⁶³ The Complex 2 showed different micrographs due to participation of carboxy in the structure as discussed earlier [Fig. 10(e)]. It can be expected that the DMC with small size and equigranular particles contribute to high activity. The small granules equably distribute in PO and allow for more activity points per unit volume, helping to couple CO_2 and PO. Based on these analyses, Complex 1 has a higher

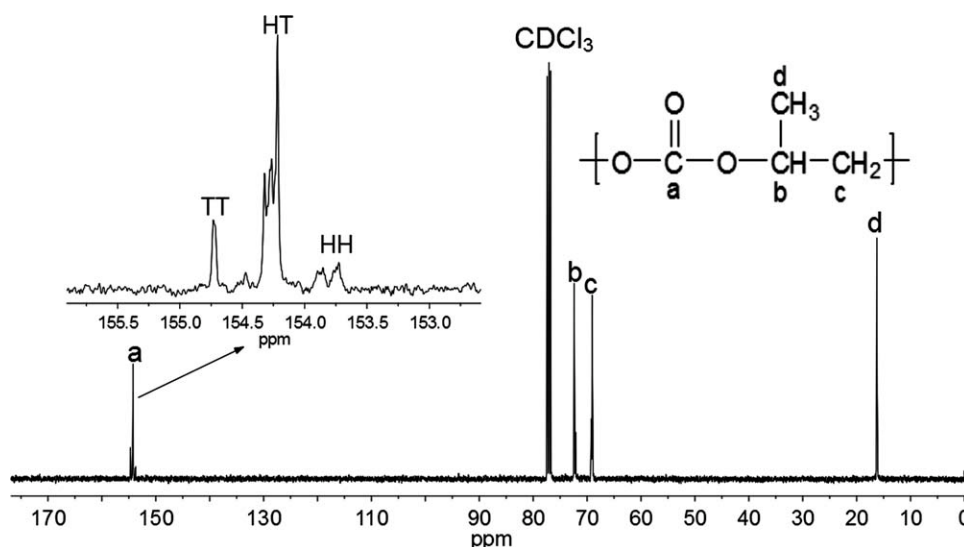


Figure 9 ^{13}C NMR spectrum of a representative sample of poly(propylene carbonate).

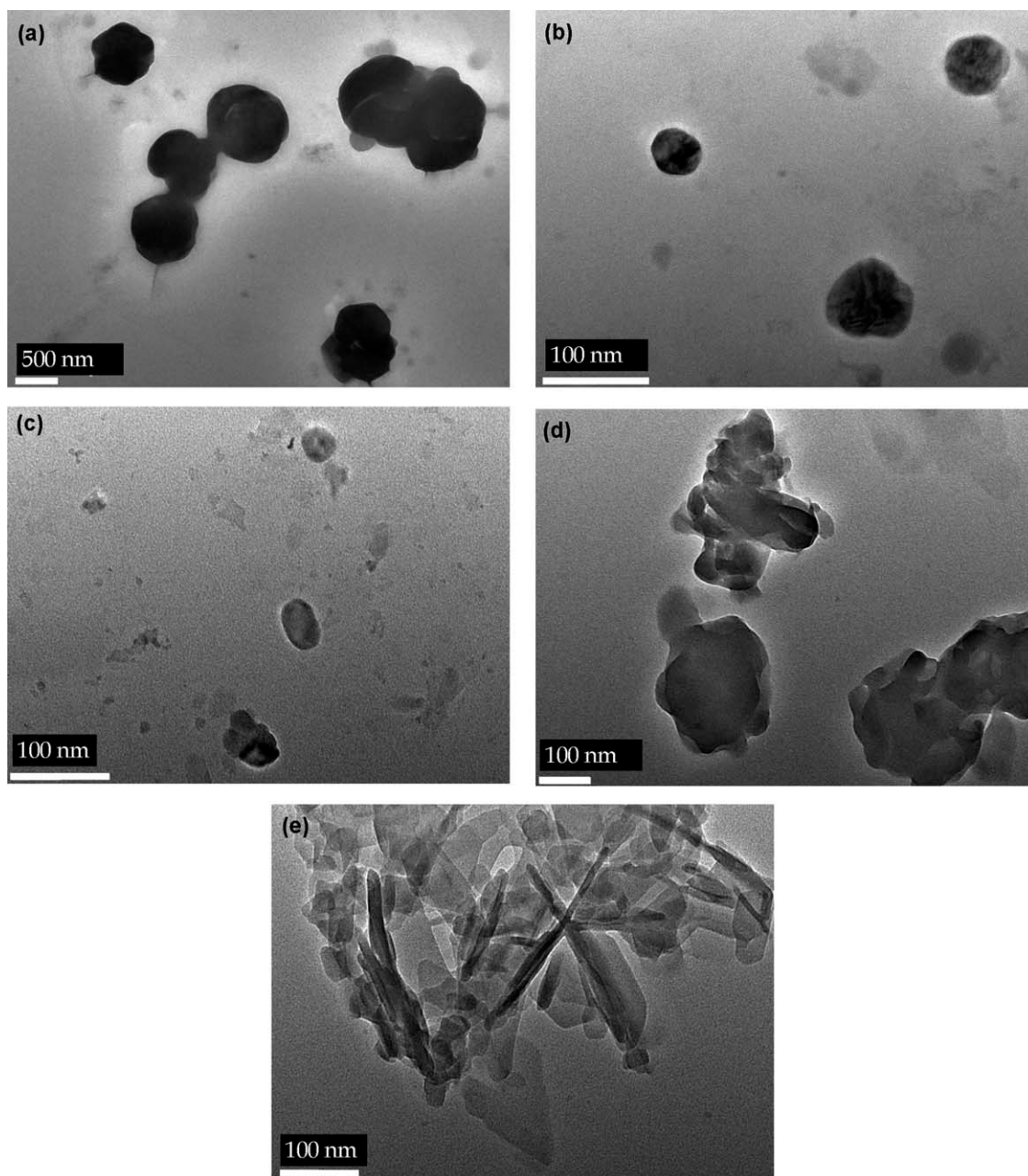


Figure 10 TEM images of nano-sized DMC: (a) Complex 1 synthesized in the solvent-based ways; (b) Complex 1 ground 14 min; (c) Complex 1 ground 24 min; (d) Complex 1 ground 40 min; and (e) Complex 2 ground 7 min.

catalytic activity than Complex 2, as well as those synthesized by the conventional solvent-based ways.

CONCLUSIONS

It has been demonstrated that high active DMC can be easily synthesized by the solvent-free grinding method. The merit is shown by (1) reconstruction into target compounds can be completed within minutes without solvent, and (2) high productivity can be achieved with ground catalyst. The grinding method reveals a clear shortcut in synthesis of DMC complexes compared with conventional solvent-

based ways. Overall, the findings improve our insight into the possibility of grinding-induced transformations and extend the application of grinding method as a convenient way to synthesize catalysts. Future work will be directed toward obtaining mechanistic insight of both complexes reconstruction and copolymerization of CO₂ and propylene oxide, as well as further improvements of the activity via optimization of the DMC and cocatalyst structure.

Analytical and Testing Center of Hainan University is acknowledged for characterization of the DMC and copolymers.

References

- Pagani, M.; Liu, Z.; LaRiviere, J. Ravelo, A. C.; Nat Geosci 2010, 3, 27.
- Matthews, H. D.; Gillett, N. P.; Stott, P. A.; Zickfeld, K. Nature 2009, 459, 829.
- Le Quéré, C.; Raupach, M. R.; Canadell, J. G.; Marland, G. Nat Geosci 2009, 2, 831.
- Leitner, W. Coord Chem Rev 1996, 153, 257.
- Walther, D.; Ruben, M.; Rau, S. Coord Chem Rev 1999, 182, 67.
- Inoue, S.; Koinuma, H.; Tsuruta, T. J Polym Sci Part C Polym Lett 1969, 7, 287.
- Inoue, S.; Koinuma, H.; Tsuruta, T. Makromol Chem 1969, 130, 210.
- Beckman, E. J. Science 1999, 283, 946.
- Kobayashi, M.; Inoue, S.; Tsuruta, T. Macromolecules 1971, 4, 658.
- Inoue, S.; Kobayashi, M.; Koinuma, H.; Tsuruta, T. Makromol Chem 1972, 155, 61.
- Kobayashi, M.; Inoue, S.; Tsuruta, T. J Polym Sci Polym Chem Ed 1973, 11, 2383.
- Kuran, W.; Pasynekiewicz, S.; Skupinska, J. Makromol Chem 1977, 178, 2149.
- Nishimura, M.; Kasai, M.; Tsuchida, E. Makromol Chem 1978, 179, 1913.
- Kuran, W.; Rokicki, A.; Wilinska, E. Makromol Chem 1979, 180, 361.
- Tsuchida, E.; Kasai, M. Makromol Chem 1980, 181, 1613.
- Soga, K.; Imai, E.; Hattori, I. Polym J 1981, 13, 407.
- Hino, Y.; Yoshida, Y.; Inoue, S. Polym J 1984, 16, 159.
- Chen, L. B.; Chen, H. S.; Lin, J. J. Macromol Sci Chem A 1987, 24, 253.
- Santangelo, J. G.; Weber, J. J.; Sinclair, R. G. US Patent 4,665,136 1987.
- Kuran, W.; Listos, T. Makromol Chem Phys 1994, 195, 977.
- Ree, M.; Bae, Y.; Jung, J. H.; Shin, T. J. J Polym Sci Polym Chem 1999, 37, 1863.
- Cheng, M.; Darling, N. A.; Lobkovsky, E. B.; Coates, G. W. Chem Commun 2000, 20, 2007.
- Nakano, K.; Nozaki, K.; Hiyama, T. Macromolecules 2001, 34, 6325.
- Allen, S. D.; Moore, D. R.; Lobkovsky, E. B.; Coates, G. W. J Am Chem Soc 2002, 124, 14284.
- Moore, D. R.; Cheng, M.; Lobkovsky, E. B.; Coates, G. W. J Am Chem Soc 2003, 125, 11911.
- Dirk, F. J. P.; Range, S.; Harder, S. Organometallics 2008, 27, 6178.
- Kember, M. R.; Knight, P. D.; Reung, P. T. R.; Williams, C. K. Angew Chem Int Ed 2009, 48, 931.
- Kember, M. R.; White, A. J. P.; Williams, C. K. Inorg Chem 2009, 48, 9535.
- Darensbourg, D. J.; Yarbrough, J. C. J Am Chem Soc 2002, 124, 6335.
- Darensbourg, D. J.; Yarbrough, J. C.; Ortiz, C.; Fang, C. C. J Am Chem Soc 2003, 125, 7586.
- Darensbourg, D. J.; Mackiewicz, R. M. J Am Chem Soc 2005, 127, 14026.
- Darensbourg, D. J.; Fitch, S. B. Inorg Chem 2008, 47, 11868.
- Paddock, R. L.; Nguyen, S. T. Macromolecules 2005, 38, 6251.
- Lu, X. B.; Shi, L.; Wang, Y. M.; Zhang, R.; Zhang, Y. J.; Peng, X. J.; Zhang, Z. C.; Li, B. J Am Chem Soc 2006, 128, 1664.
- Ren, W. M.; Liu, Z. W.; Wen, Y. Q.; Zhang, R.; Lu, X. B. J Am Chem Soc 2009, 131, 11509.
- Kember, M. R.; White, A. J. P.; Williams, C. K. Macromolecules 2010, 43, 2291.
- Herold, R. J. US Patent 3,278,459, 1966.
- Kuyper, J.; Struyckenkamp, V. S. US Patent 4,472,560, 1984.
- Kruper, W. J.; Swart, D. J. US Patent 4,500,704, 1985.
- Chen, L. B. Makromol Chem Macromol Symp 1992, 57, 75.
- Soltani-Ahmadi, A.; Le-Khac, B.; Bullano, G. A. US Patent 5,900,384, 1999.
- Lu, L. B.; Huang, K. L. Polym Int 2005, 54, 870.
- Herold, R. J.; Livigni, R. A. Polym Prepr (Am Chem Soc Div Polym Chem) 1972, 13, 545.
- Herold, R. J.; Livigni, R. A. Adv Chem Ser 1973, 128, 208.
- Herold, R. J. Macromol Synth 1974, 5, 9.
- Livigni, R. A.; Herold, R. J.; Elmer, O. C.; Aggarwal, S. L. ACS Symp Ser 1975, 6, 20.
- Kuyper, J.; Boxhoon, G. J Catal 1987, 105, 163.
- Kim, I.; Byun, S.-H.; Ha, C.-S. J Polym Sci Part A Polym Chem 2005, 43, 4393.
- Urakaev, F. K.; Boldyrev, V. V. Powder Technol 2000, 107, 93.
- Urakaev, F. K.; Boldyrev, V. V. Powder Technol 2000, 107, 197.
- Juhász, A. Z. Aufbereitungs-Technik 1974, 10, 558.
- Milosevic, S.; Ristic, M. M. Sci Sinter 1998, 30, 29.
- Briottet, L.; Jonas, J. J.; Montheillet, F. Acta Mater 1996, 44, 1665.
- Juhász, A. Z. Colloids Surf A 1998, 141, 449.
- Takacs, L. Prog Mater Sci 2002, 47, 355.
- Savolainen, M.; Kogermann, K.; Heinz, A.; Aaltonen, J.; Peltonen, L.; Strachan, C.; Yliruusi, J. Eur J Pharm Biopharm 2009, 71, 71.
- Verdaguer, M.; Bleuzen, A.; Marvaud, V.; Vaissermann, J.; Seuleiman, M.; Desplanches, C.; Sculler, A.; Train, C.; Garde, R.; Gelly, G.; Lomenech, C.; Rosenman, I.; Veillet, P.; Cartier, C.; Villain, F. Coord Chem Rev 1999, 190-192, 1023.
- Kim, H. S.; Kim, J. J.; Lee, S. D.; Lah, M. S.; Moon, D.; Jang, H. G. Chem Eur J 2003, 9, 678.
- Huang, Y.-J.; Zhang, X.-H.; Hua, Z.-J.; Chen, S.-L.; Qi, G.-R. Macromol Chem Phys 2010, 211, 1229.
- Lee, S.; Baek, S. T.; Anas, K.; Ha, C.-S.; Park, D.-W.; Lee, J. W.; Kim, I. Polymer 2007, 48, 4361.
- Lee, I. K.; Ha, J. Y.; Cao, C.; Park, D.-W.; Ha, C.-S.; Kim, I. Catal Today 2009, 148, 389.
- Chisholm, M. H.; Navarro-Llobet, D.; Zhou, Z. Macromolecules 2002, 35, 6494.
- Yi, M. J.; Byun, S.-H.; Ha, C.-S.; Park, D.-W.; Kim, I. Solid State Ionics 2004, 172, 139.